Comparison of NWP based nowcasting (AROME) with classical system

III. Results

RC - LACE stay report

by Mirela Pietrisi
Supervisors: Christoph Wittmann, Florian Meier and Yong Wang

Results from the feature - based method: Method for Object-Based Diagnostic Evaluation (MODE)

As discussed in the previous reports, the traditional metrics do not provide specific information about the types of errors (displacement, location, shape) and because of the double-penalty issue, to obtain the diagnostics in which a forecast was good or bad is difficult. Therefore, two categories of spatial techniques using different ways of evaluating the model skill were applied: the filtering (neighborhood verification) and feature-based methods.
The feature-based methods are used to investigate how well the forecast captures spatial patterns. The method applied in this study is MODE (**M**ethod for **O**bject-**B**ased **D**iagnostic **E**valuation). Using the MODE approach described by Davis et al. (2006a, b) we evaluated the precipitation forecasts.
Briefly, the following steps were taken into account:

- The objects (defined as spatial regions of interest) in both fields (forecast and observed) were identified. This is based on a convolution and thresholding process, which involves choosing the convolution radius (radius of influence) and the convolution threshold;

- The object attributes (which measure the spatial features of the objects) were computed. MODE computes many attributes that can be classified into two categories. The first category of attributes is for single objects without reference to any other object (for ex: object area). The second type of attribute is for object pairs (for ex: centroid difference, angle difference, union area, intersection area, symmetric difference). These attributes are important in evaluating the ability of a forecast to predict the observed objects features;

- The fuzzy logic engine process, which is part of MODE, was applied to identify similarities between forecast and observed objects. Using the fuzzy engine approach, the objects attributes were merged (refers to associating objects in the same field) and matched (refers to associating objects in different fields). The matched forecast and observed objects are referred to as pairs and the merged objects are referred to as clusters;

- Summary statistics describing the objects attributes are produced and used to identify the strength or the weakness of the forecast;

- Summarize the performance of the forecasts across many cases;

More information about the methods used by MODE to identify and verify objects can also be found in Davis et al. (2009) and Brown et al. (2007).

Different combination of parameters can be applied, therefore selecting the optimal configuration which will best capture the interest features is an iterative process. The main challenge is to define the forecast and observed objects depending on the kind of forecast interest situation (Mittermaier, 2013). The way objects are identified is affected by the selection of two parameters: the convolution radius (which determines the smoothing process) and the precipitation threshold.

Firstly, the forecast performance across scales was examined by investigating the performance statistics as a function of convolution radius and threshold for AROME and INCA (not shown). Therefore, different convolution radius and thresholds were applied to both forecast and observation field. Low values of radius and threshold produce many objects and the number of objects decreases when one of the parameter is increased. From these plots we selected the reasonable values of the two main parameters (convolution radius and threshold).

Model dataset

The numerical forecasts generated by AROME Nowcasting system are provided on a regular latitude - longitude grid, with 2.5 km horizontal resolution and 90 vertical levels. The hourly cycling 3D-Var system assimilates radar data as well as other types of observations from OPLACE system and local data base. The gridded precipitation analysis from INCA are assimilated through latent heat nudging technique. For more details about the design and the implementation of the AROME Nowcasting system at ZAMG, see [1].

INCA (**I**ntegrated **N**owcasting through **C**omprehensive **A**nalysis) is operationally run on a 3D grid with 1 km horizontal resolution and vertical around 100 - 200 m. The nowcasting system incorporates synop observations, radar, satellite and high resolution topographic data. In this study, two datasets of precipitation forecasts are used: one set provided by INCA based extrapolation system (classical correlation-based motion vectors) reffered further as **INCA-N** - and another set from INCA NWP based system (after 1-2 h forecast time, INCA-N is merged into AROME forecast), reffered further as **INCA-O**.

Observation

INCA analysis dataset is used for verification. To be read it by MODE (can handle gridded input data in GRIB1 or GRIB2 and netCDF classic format), INCA analysis files had to be converted into the required format. First, the 15 minutes precipitation files are hourly cumulated. Second, the files are converted from text-based data files into netCDF format by using NCL software. The observations are interpolated into AROME grid through Cressman method.

Case study: 02^{nd} of July 2016

With a low pressure feature over UK, a high pressure feature in western Rusia and a broad ridge over Mediterranean Sea and south-western Europe, the second day of the warmest month in records from 1881 to 2016 (NOAA's climate report, 2017) was presenting an unusual reversed omega pattern over Europe. During the day, an active cold front streched from Scandinavia to the Alps swept the Central and Northern Europe bringing wet weather with showers, moderate rain, thunderstorms and wind gusts. Figure 1 shows the ECMWF analyses for mean sea level pressure + temperature at 850 hPa fields (left) and geopotential + temperature at 500 hPa (right).

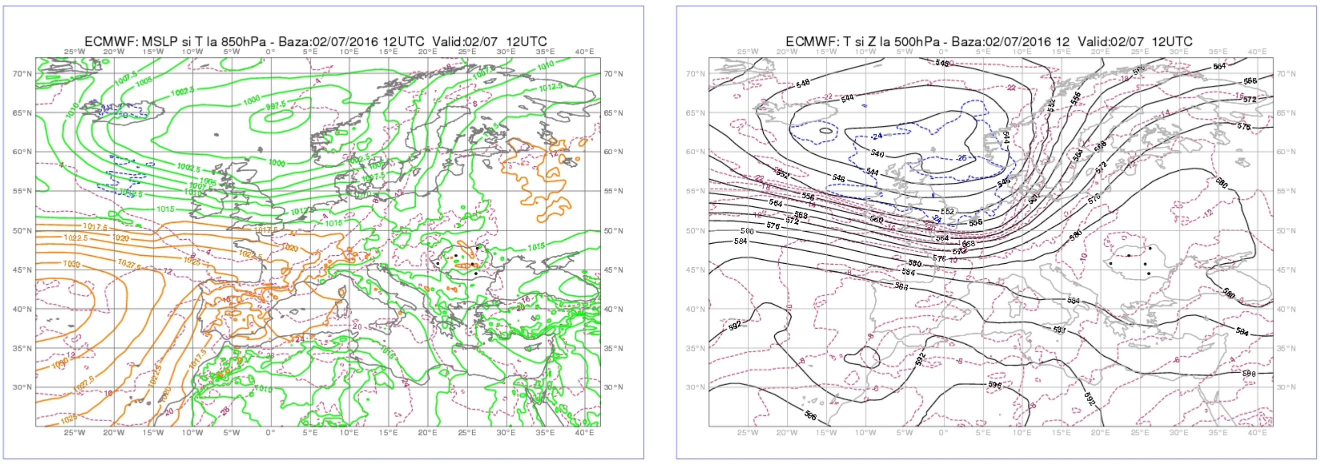

Figure 1: ECMWF, synoptic charts: MSLP + T at 850 hPa (left) and Z + T at 500 hPa (right)

MODE was applied for three combination of convolution radius (R = 2, 4, 5 grid units) and convolution thresholds ($T \geq =2.0$, $\geq = 4.0$, $\geq = 6.0$). Multiple convolution radii and thresholds were processed using the *quilt* entry, but only the results obtained for $T \geq =2.0$ and $R = 2$ grid units are presented.

Figures 2, 5 and 7 show the objects created by MODE from the hourly forecasts and observation fields of AROME, INCA-O and INCA-N simulations initialized at 13 UTC, valid at 14 UTC, 17 UTC and 19 UTC. Note that the objects identied by MODE in the observation fields are approximately similar for all simulations. It must be taken into account that depending on the forecast field, the comparison between the observed and forecast fields may identify different ways to match clusters objects. Similar colors between the fields indicate matched objects, royal blue color meaning unmatched objects.

Figures 3, 6 and 8 show the forecast objects with the outlines of the observation objects overlaid of AROME, INCA-O and INCA-N simulations initialized at 13 UTC, valid at 14 UTC, 17 UTC and 19 UTC. From the figures presented below, it can be noticed that the forecasted area of the objects simulated by AROME is larger than the observed one. Regarding the INCA simulations, there is a good match between the forecast and the observed areas, in the first hour. For INCA-N simulations, starting with the second forecast hour, it is visible that matching the forecast objects with observation outlines is more difficult.

Figure 4 shows an example of MODE simple and cluster attributes of AROME, INCA-O and INCA-N simulations initialized at 13 UTC, valid at 14 UTC. The convex hull outlines for clusters (black lines surrounding the objects), simple and cluster object numbers are also included. This kind of information is obtained for all the simulations (not shown).

To quantify the similarity of the objects, the total interest value (TTI) is computed for each object pair. The precipitation objects were matched if $TTI \geq 0.7$.

To assess the forecast accuracy, several diagnostic MODE measures were evaluated. One of them is the symmetric difference. This attribute can be a good indicator of forecast quality, since it measures the area that's inside at least one of the objects. If the value is small, it means that the two objects nearly coincide. For the INCA simulations, the smallest symmetric differences were found in the first two hours, while for AROME's simulations the values were small at the forecast hours 3, 5 and 6. The result may indicate a problem with the location of the storms.

Another attribute available through MODE is the frequency bias, computed as the area ratio of identified forecast objects to identified observed objects. The same conclusion can be drawn with regard to the symmetric difference attribute.

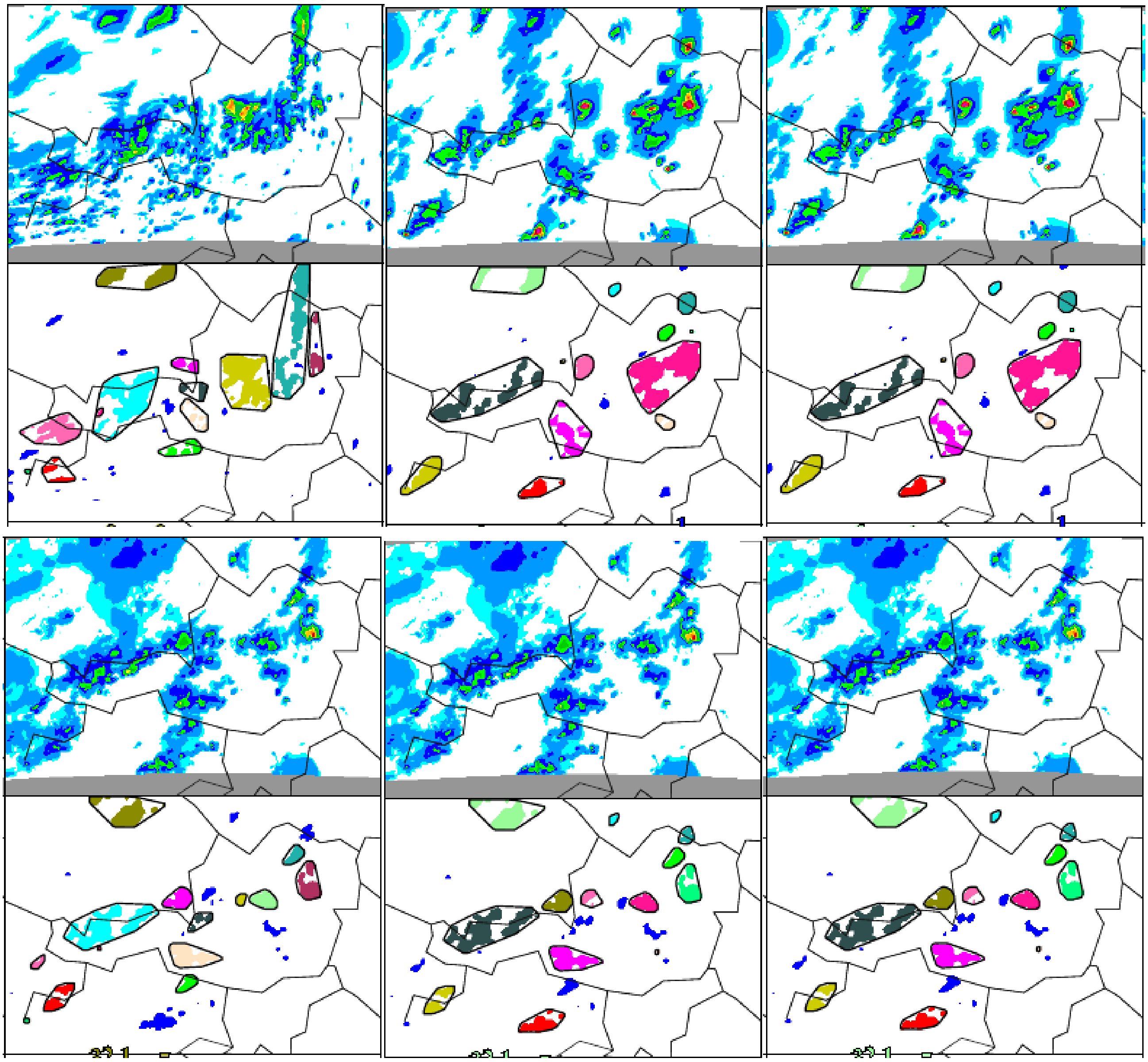

Figure 2: MODE precipitation objects defined using a convolution threshold of 2.0 mm/h and a smoothing radius of 2 grid square for AROME (left), INCA-O (middle), INCA-N (right) simulations initialized at 13 UTC and associated analysis field (bottom panel) for 02^{th} of July, valid at 14 UTC. Similar colors between the fields indicate matched objects

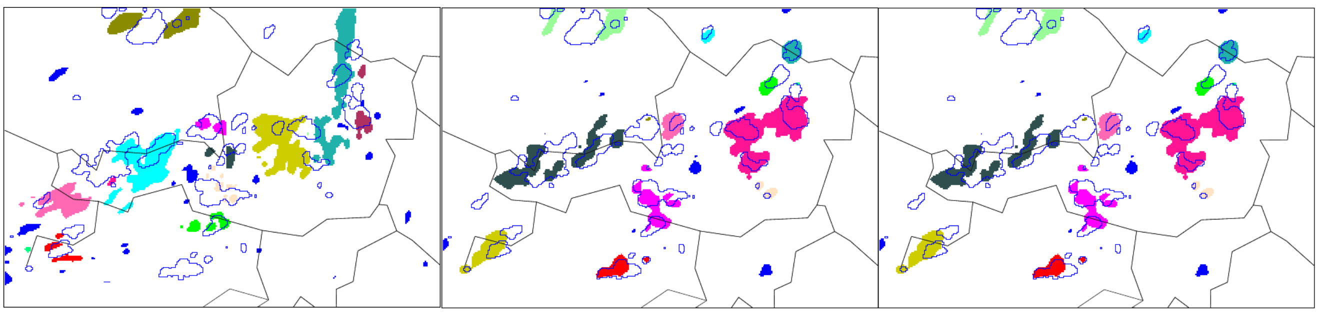

Figure 3: MODE forecast objects with the outlines of the observation objects overlaid defined using a convolution threshold of 2.0 mm/h and a smoothing radius of 2 grid square for AROME (left), INCA-O (middle), INCA-N (right) simulations initialized at 13 UTC for 02^{th} of July, valid at 14 UTC

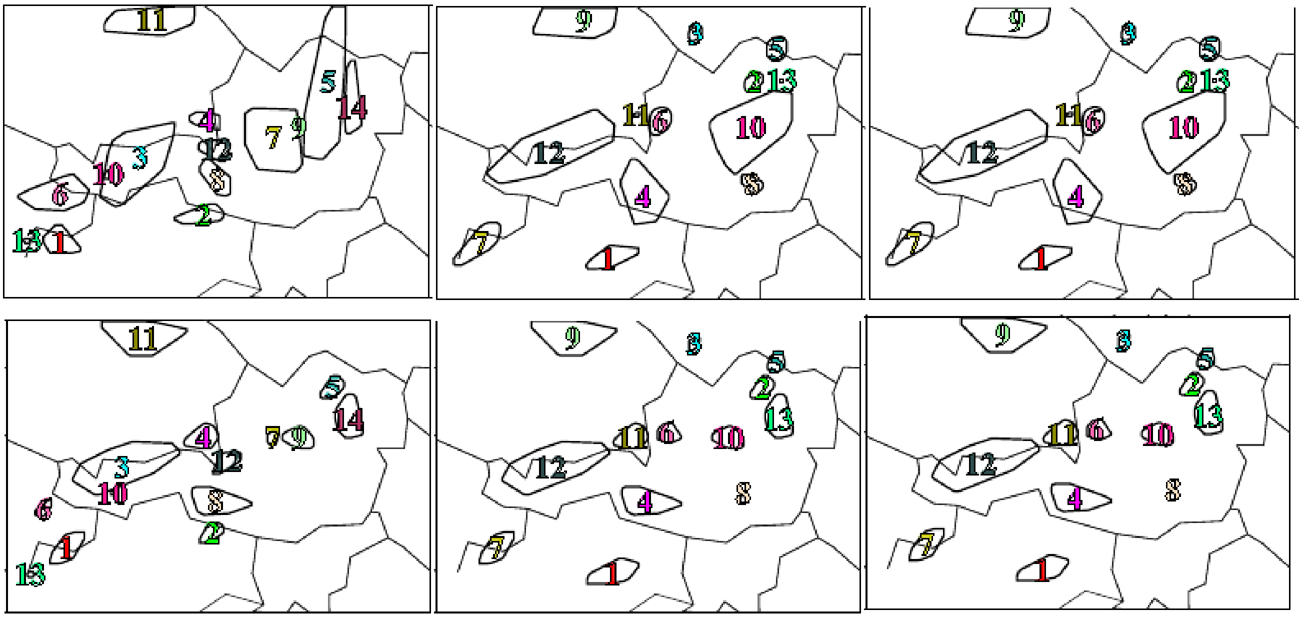

CLUS PAIR	CEN DIST	ANG DIFF	FCST AREA	OBS AREA	INTER AREA	UNION AREA	SYMM DIFF	FCST INT 50	OBS INT 50	FCST INT 90	OBS INT 90	TOT INTR
1	7.48	83.80	160	251	24	387	363	3.45	2.71	7.29	4.91	0.8515
2	5.09	29.44	211	149	84	276	192	3.76	3.70	10.08	7.25	0.9870
3	16.21	30.58	1233	1116	451	1898	1447	3.48	3.53	8.67	7.17	0.9976
4	4.56	33.57	153	288	91	350	259	3.88	4.55	7.90	10.12	0.9573
5	7.41	35.31	1271	172	139	1304	1165	4.77	5.52	13.87	15.81	0.8879
6	14.24	36.14	596	67	43	620	577	3.38	2.87	6.36	8.63	0.8824
7	11.78	58.99	1221	64	64	1221	1157	5.05	3.87	19.01	8.84	0.8524
8	5.91	42.89	129	464	64	529	465	3.55	3.31	6.94	7.00	0.9037
9	3.99	73.70	2	249	2	249	247	2.49	3.94	2.50	9.89	0.8168
10	3.21	81.82	26	8	1	33	32	3.17	4.37	4.81	7.27	0.7753
11	9.04	11.47	613	553	43	1123	1080	4.49	2.78	9.85	3.94	0.8717
12	5.93	46.96	127	121	32	216	184	3.49	2.71	5.76	3.78	0.9842
13	14.31	2.97	14	16	0	30	30	3.53	2.92	7.36	5.26	0.7356
14	5.00	6.26	216	366	110	472	362	5.03	6.64	13.25	24.70	0.9703

CLUS PAIR	CEN DIST	ANG DIFF	FCST AREA	OBS AREA	INTER AREA	UNION AREA	SYMM DIFF	FCST INT 50	OBS INT 50	FCST INT 90	OBS INT 90	TOT INTR
1	4.24	3.31	248	312	183	377	194	7.56	4.01	33.17	10.01	0.9993
2	9.59	2.96	129	172	56	245	189	3.53	5.52	13.82	15.81	0.9931
3	2.47	7.54	74	51	36	89	53	4.56	3.97	10.10	6.34	0.9844
4	7.04	55.12	507	464	233	738	505	3.50	3.31	8.68	7.00	0.9753
5	0.30	1.21	214	124	124	214	90	7.54	2.90	33.23	4.21	0.9675
6	5.52	81.67	245	103	74	274	200	5.66	3.64	31.69	8.94	0.9057
7	13.85	5.14	427	251	119	559	440	4.31	2.71	7.49	4.91	0.9701
8	6.96	73.44	95	9	9	95	86	4.92	3.27	20.50	4.43	0.8438
9	8.07	9.09	441	553	73	921	848	3.26	2.78	8.13	3.94	0.9391
10	16.02	52.00	1608	249	249	1608	1359	5.20	3.94	17.37	9.89	0.8731
11	7.52	4.04	9	288	9	288	279	3.21	4.55	3.75	10.12	0.8721
12	2.18	3.88	1102	1116	414	1804	1390	4.30	3.53	9.21	7.17	1.0000
13	18.94	82.94	6	366	2	370	368	5.34	6.64	5.98	24.70	0.8121

CLUS PAIR	CEN DIST	ANG DIFF	FCST AREA	OBS AREA	INTER AREA	UNION AREA	SYMM DIFF	FCST INT 50	OBS INT 50	FCST INT 90	OBS INT 90	TOT INTR
1	4.24	3.31	248	312	183	377	194	7.55	4.01	33.16	10.01	0.9993
2	9.59	2.96	129	172	56	245	189	3.52	5.52	13.82	15.81	0.9931
3	2.47	7.54	74	51	36	89	53	4.56	3.97	10.09	6.34	0.9844
4	7.04	55.12	507	464	233	738	505	3.50	3.31	8.68	7.00	0.9753
5	0.31	1.17	213	124	124	213	89	7.67	2.90	33.23	4.21	0.9679
6	5.52	81.67	245	103	74	274	200	5.66	3.64	31.69	8.94	0.9057
7	13.85	5.14	427	251	119	559	440	4.30	2.71	7.48	4.91	0.9701
8	6.96	73.44	95	9	9	95	86	4.93	3.27	20.49	4.43	0.8438
9	8.07	9.09	441	553	73	921	848	3.26	2.78	8.12	3.94	0.9391
10	16.02	52.00	1608	249	249	1608	1359	5.19	3.94	17.37	9.89	0.8731
11	7.52	4.04	9	288	9	288	279	3.21	4.55	3.74	10.12	0.8721
12	2.16	3.89	1101	1116	413	1804	1391	4.30	3.53	9.21	7.17	1.0000
13	18.94	82.94	6	366	2	370	368	5.33	6.64	5.97	24.70	0.8121

Figure 4: Example of MODE cluster object information defined using a convolution threshold of 2.0 mm/h and a smoothing radius of 2 grid square for AROME (left), INCA-O (middle), INCA-N (right) simulations initialized at 13 UTC for 02^{th} of July, valid at 14 UTC

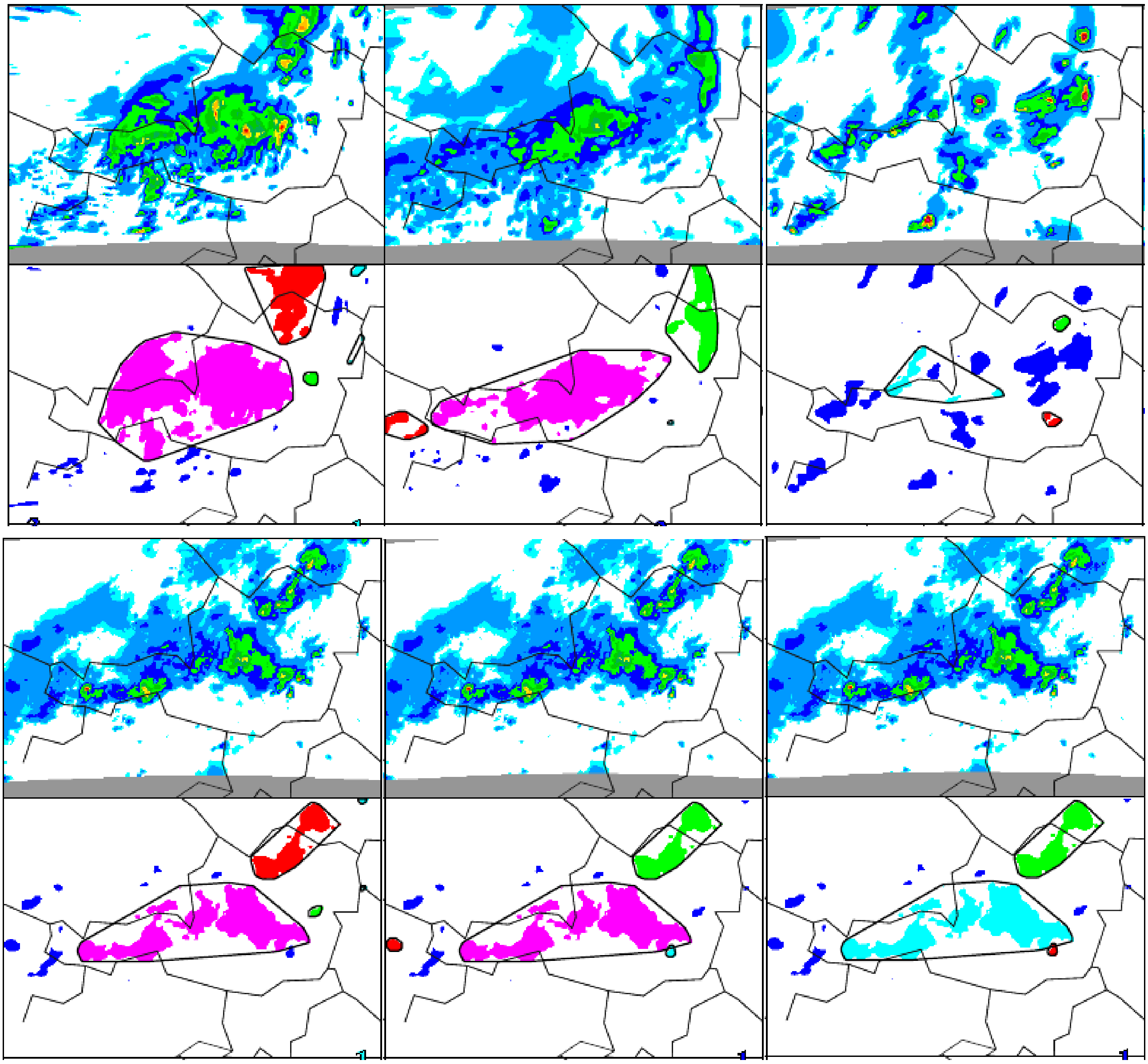

Figure 5: MODE precipitation objects defined using a convolution threshold of 2.0 mm/h and a smoothing radius of 2 grid square for AROME (left), INCA-O (middle), INCA-N (right) simulations initialized at 13 UTC and associated analysis field (bottom panel) for 02^{th} of July, valid at 17 UTC. Similar colors between the fields indicate matched objects

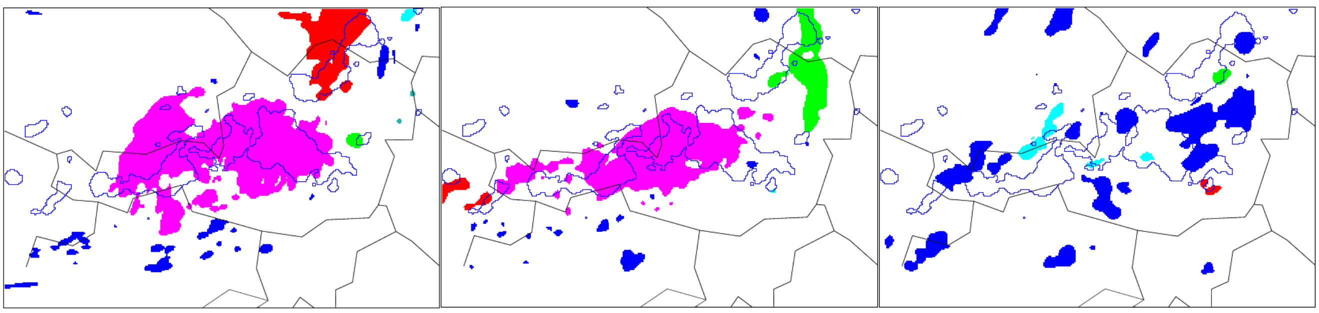

Figure 6: MODE forecast objects with the outlines of the observation objects overlaid defined using a convolution threshold of 2.0 mm/h and a smoothing radius of 2 grid square for AROME (left), INCA-O (middle), INCA-N (right) simulations initialized at 13 UTC for 02^{th} of July, valid at 17 UTC

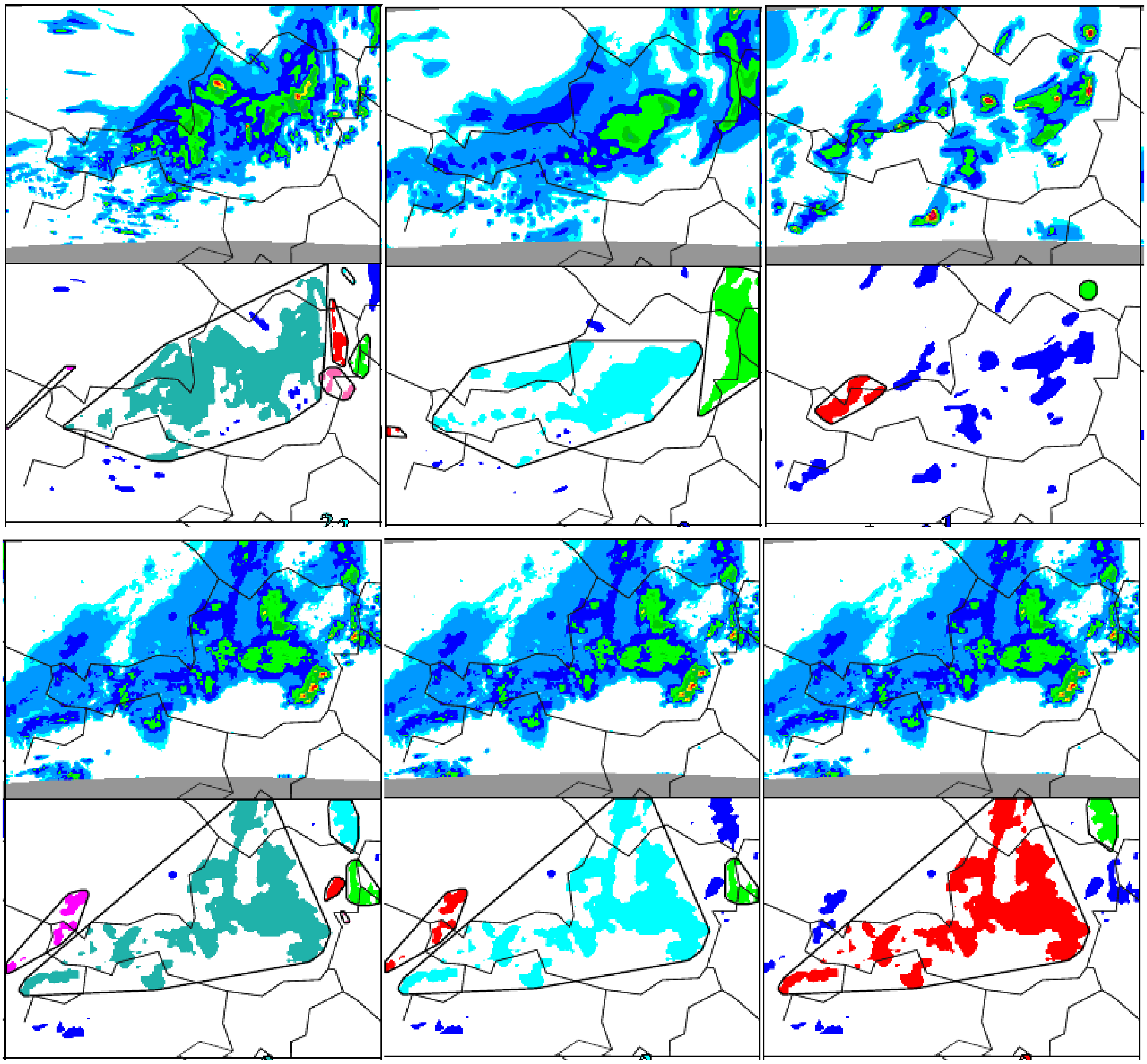

Figure 7: MODE precipitation objects defined using a convolution threshold of 2.0 mm/h and a smoothing radius of 2 grid square for AROME (left), INCA-O (middle), INCA-N (right) simulations initialized at 13 UTC and associated analysis field (bottom panel) for 02^{th} of July, valid at 19 UTC. Similar colors between the fields indicate matched objects

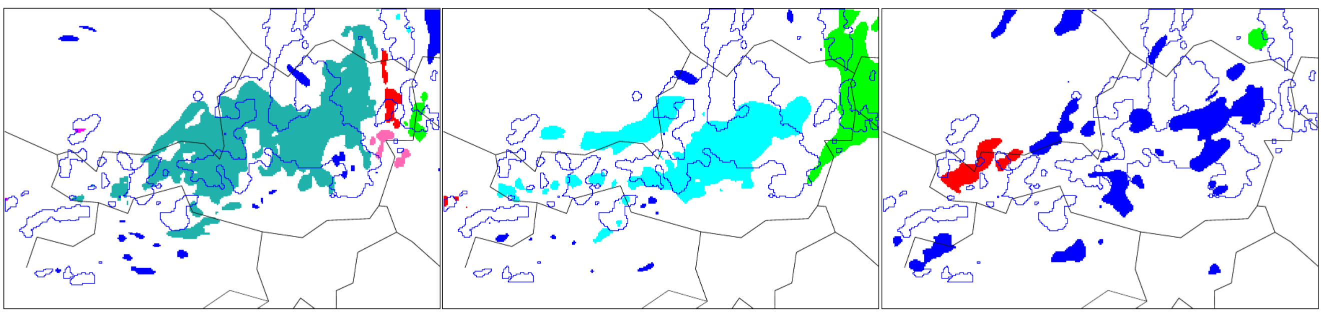

Figure 8: MODE forecast objects with the outlines of the observation objects overlaid defined using a convolution threshold of 2.0 mm/h and a smoothing radius of 2 grid square for AROME (left), INCA-O (middle), INCA-N (right) simulations initialized at 13 UTC for 02^{th} of July, valid at 19 UTC

Using the MODE-Analysis tool, the results obtained by MODE were summarized and aggregated. Figures 9 and 10 show the total number of simple objects (regardless if they are matched or unmatched) identified by MODE, summed by forecast lead time for each temporal aggregation, using a smoothing radius of 2 grid square and convolution threshold of 2.0 mm/h and 6.0 mm/h.

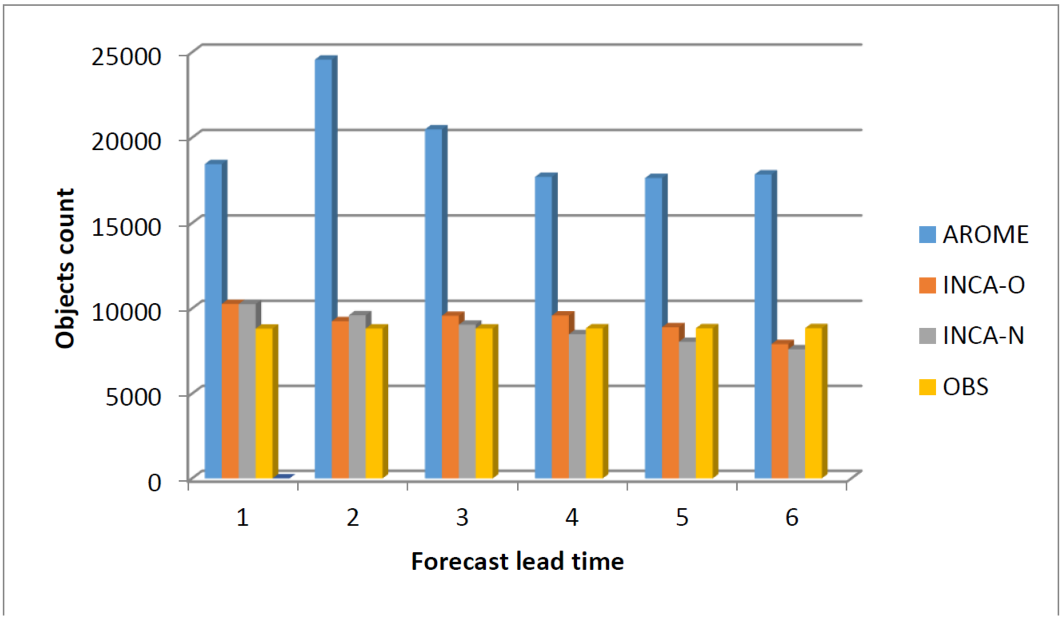

Figure 9: Total object counts by lead time for AROME (blue), INCA-O (orange), INCA-N (grey) forecasts and analysis objects - OBS (yellow) fields aggregated across summer using a threshold of 2.0 mm/h and a smoothing radius of 2 grid square

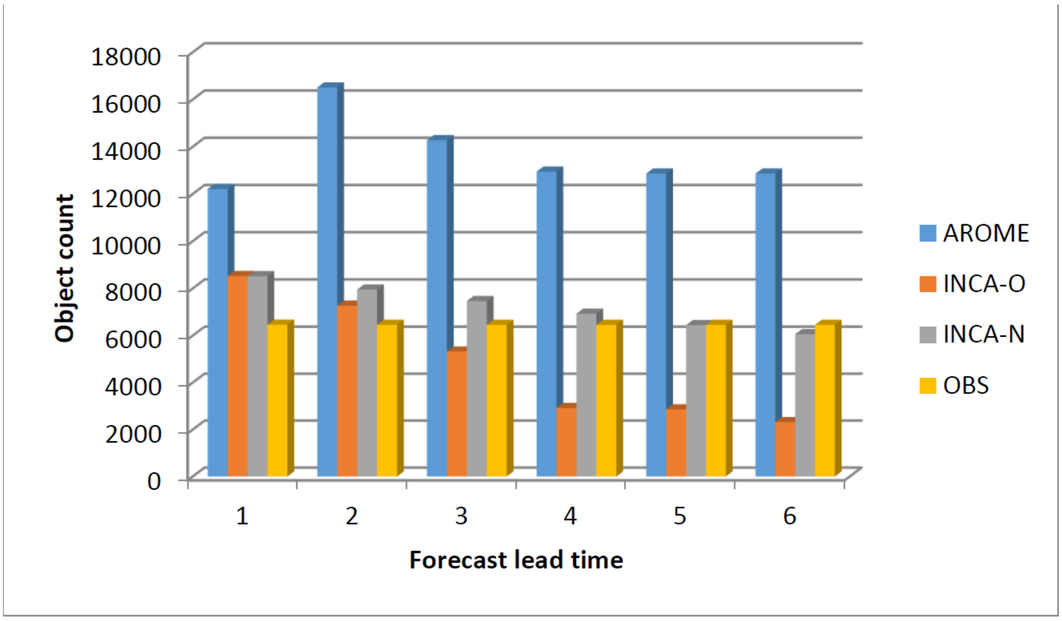

Figure 10: Total object counts by lead time for AROME (blue), INCA-O (orange), INCA-N (grey) forecasts and analysis objects - OBS (yellow) fields aggregated across summer using a threshold of 6.0 mm/h and a smoothing radius of 2 grid square

Regardless of lead time, the number of the precipitation objects identified by MODE in the AROME forecast field is substantially higher than the number of the observed objects. For all the convolution radius and thresholds, the total object counts for the summer aggregation is larger for AROME than for the INCA systems (not shown).

Summary

The feature-based method, MODE (which is part of the **M**odel **E**valuation **T**ool), described by Davis et al (2006a, b) was used in this study. MODE provides diagnostic information (about the nature of forecast errors) that is meaningful for the high-resolution NWP applications. It was applied for the evaluation of the hourly precipitation forecasts provided by AROME, INCA-N and INCA-O for July 2016 and January 2017. Taking into account the fact that our synoptic interest features are related to mesoscale precipitation systems, only the results from July 2016 are presented, as well as a case study from 02^{nd} of July. Different combination of parameters (convolution radius and convolution thresholds) were applied to both forecast and observation fields for all datasets. As it was mentioned before, selecting the optimal configuration (all the configurations were post-processed to a 2.5 km common grid) is an iterative process. The statistics of objects attributes from MODE were examined to identify the correlations and the differences between the identified objects.
In general (the results obtained by the aggregation of the MODE output) AROME Nowcasting simulates more objects than INCA systems with respect to observed objects. Regardless if the objects are matched, clusterized or unmatched, for all the convolution radius and convolution thresholds tested, AROME overpredicted the precipitation systems.

Selected results for the 02^{nd} of July 2016 were presented. It was noticed that the forecast area of the objects simulated by AROME was larger than the observed one. For the first lead time, INCA simulations showed a good match between the forecast and observed areas. Starting with the second forecast lead time, INCA-N simulations showed that matching the forecast objects with observation outlines is more difficult. To assess the forecast accuracy, the symmetric difference was evaluated (if the value is small it means that the objects nearly coincide). For INCA-O, the smallest symmetric differences were found for the first two forecast hours. The increase of the attribute values with lead time is noticed. For AROME's simulations the small values were registrated for the forecast lead time 3, 5 and 6. These results may indicate a problem of the model with the location of any individual mesoscale system.

Sensitivity to initial state

Case: 02^{nd} of July 2016

The aim of the experiments was to understand the spin up oscillations in AROME Nowcasting system occured in the first hour of simulations. AROME Nowcasting was hourly run for this case with a 3DVAR radar assimilation and latent heat nudging.

ECHKEVO tool was used to compute the time evolution of the pressure and temperature fields in 4 points of the domain which are specified in detail in Table 1, at the lowest model level. Figure 11 shows the AROME domain (576 x 900 grid points, L90, $\Delta x = 1.2$ km).

Experiment names:

- EXP1 - AROME "open loop"
- EXP2 - AROME cycled (+ filtering)
- EXP3 - AROME + IAU cycling configuration

Figures 12 and 13 show the pressure evolution while Figures 14 and 15 show the temperature evolution at the lowest model level, for the all 4 points, tstep = 150 sec period.

Note the spurious oscillations seen not only for the points which are situated in the mountain area. Although these oscillations are more pronounced in the mountain grid points, they are also present for point 1 (Vienna). The experiment EXP3 is not able to diminish the noise from the analysis.
Regarding the results showing the temperature evolution, they are much less noisy, for all the experiments.

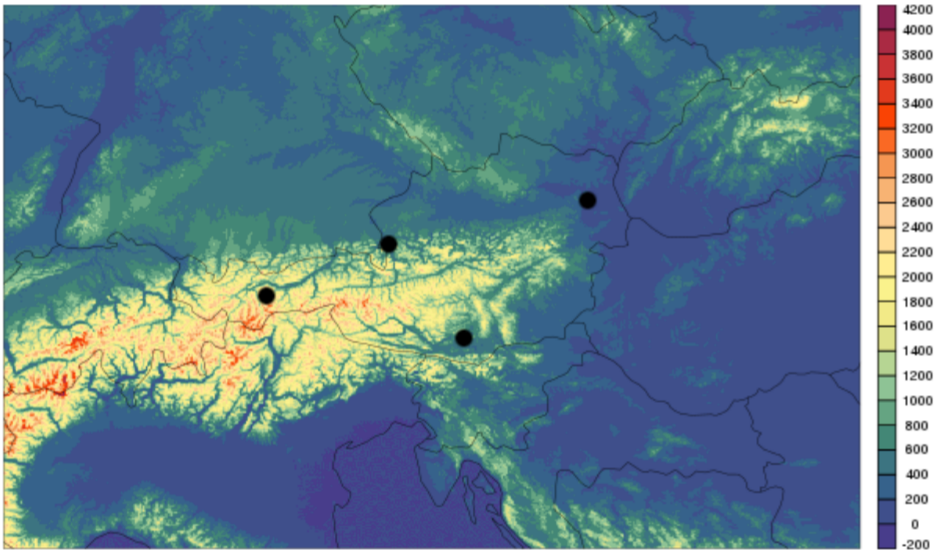

Figure 11: AROME domain: 576 x 900 grid points, L90, $\Delta x = 1.2$ km. The grid points marked by black dots are used by ECHKEVO tool to produce the output

Summary

The results showing the pressure evolution need further investigation. The oscillations are present for all the experiments, for all 4 points (although there are not so pronounced for point nb.1, Vienna). For this case, the experiment EXP3 registered the highest amplitudes comparing with the other two experiments. The question why EXP3 produces large amplitudes gravity waves needs to be explored.

The results showing the temperature evolution are less noisy. Yet, in the first 20 sec, some small oscillations are present for EXP1 and EXP2. The experiment EXP3 has a different behaviour which is kept for all 4 points. The temperature field is much better in balance after the IAU cycling configuration is applied.

Point No	LAT	LON
1. Vienna	48.2133	16.6752
2. Innsbruck	48.2669	11.3983
3. Klagenfurt	46.6326	14.3186
4. Salzburg	47.8077	13.0609

Table 1. Coordinates of points used for Echkevo output

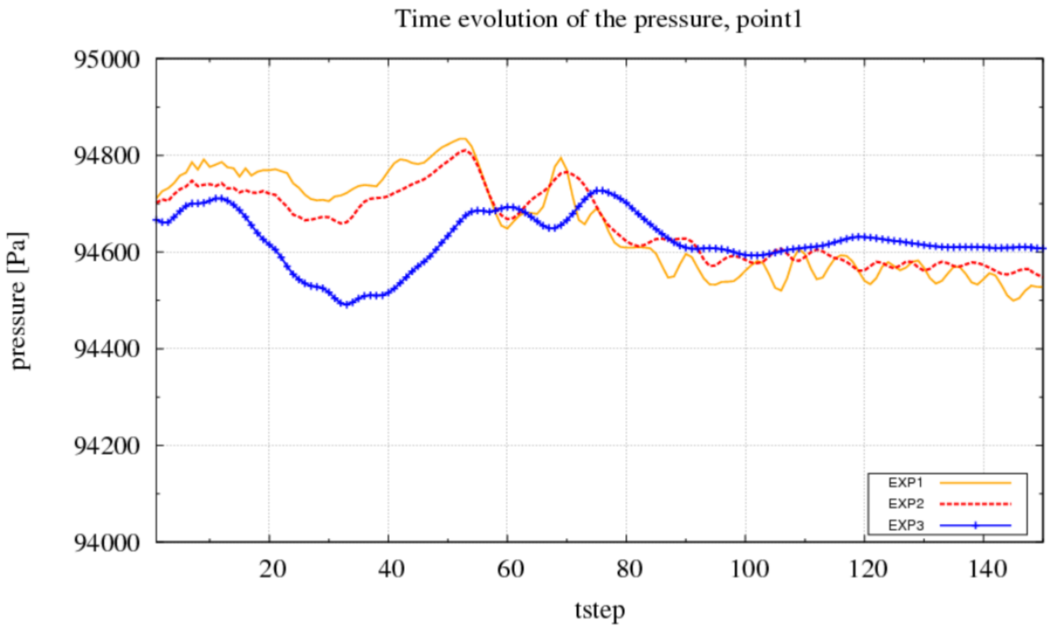

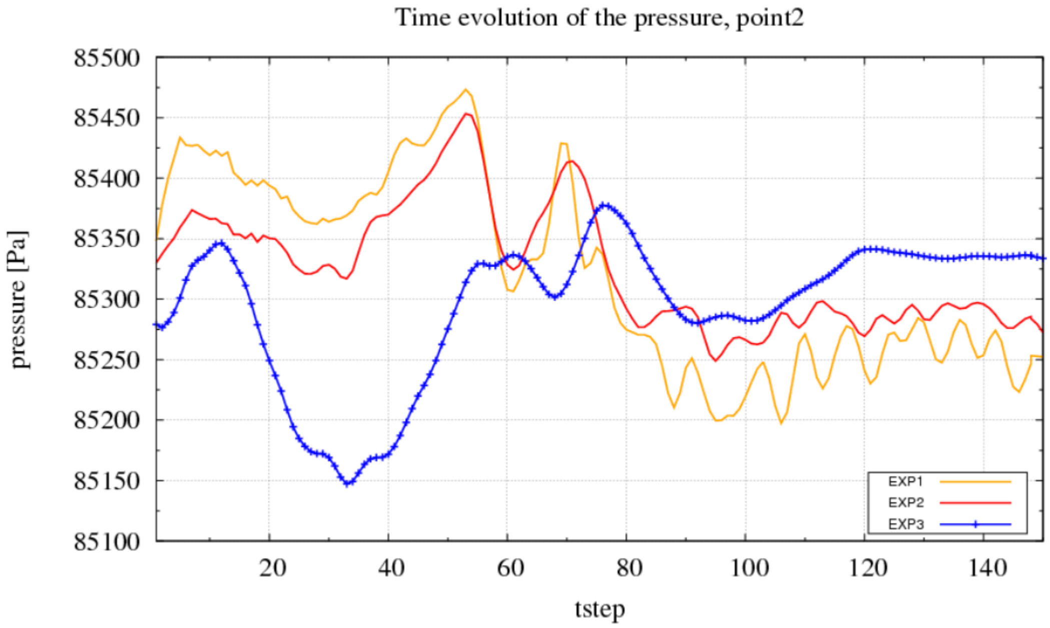

Figure 12: Time evolution of the pressure for Vienna and Innsbruck

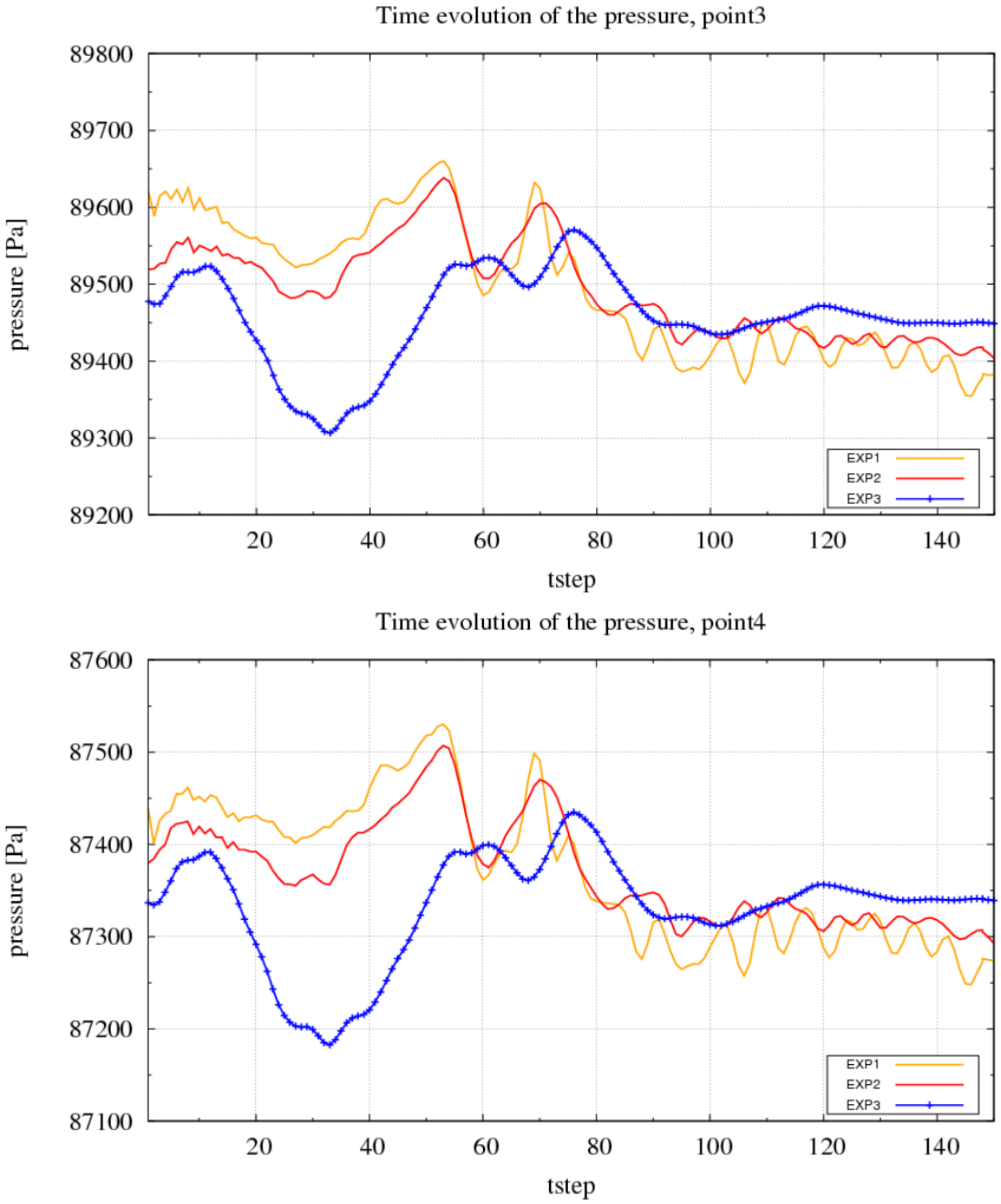

Figure 13: Time evolution of the pressure for Klagenfurt and Salzburg

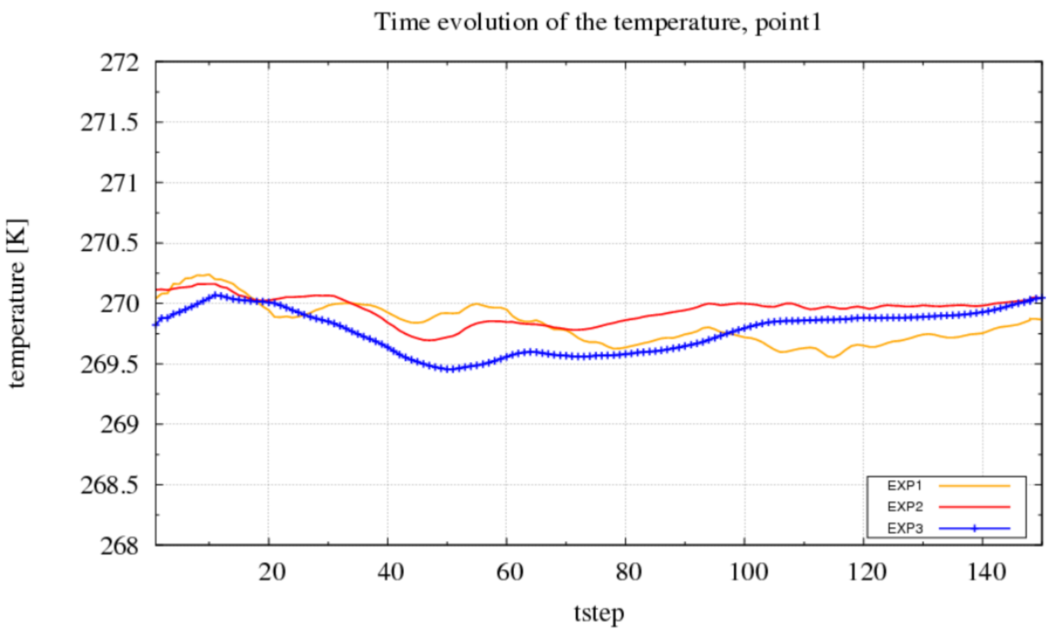

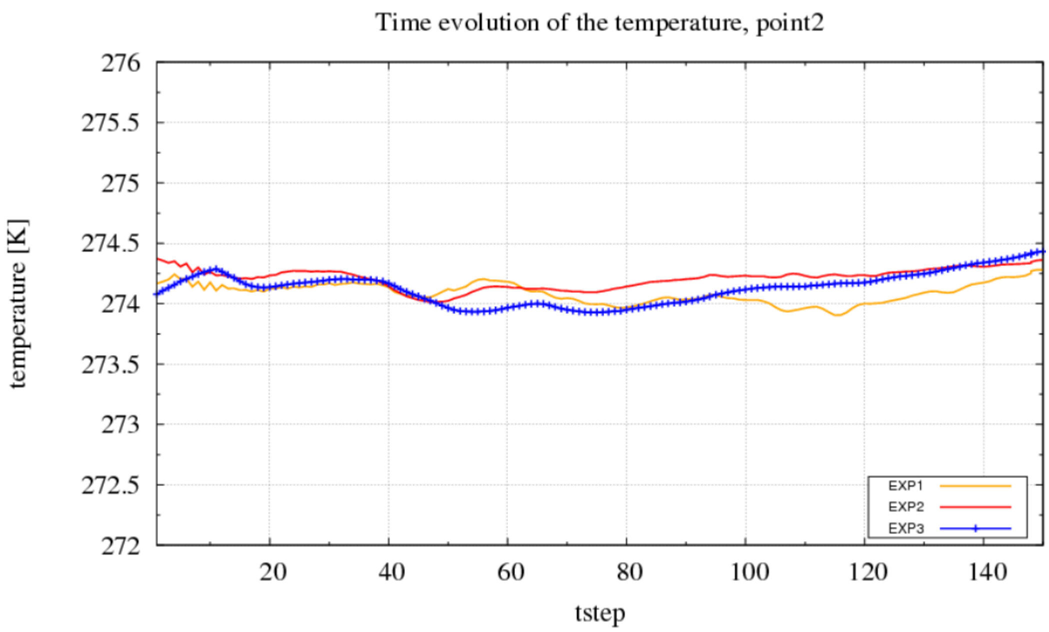

Figure 14: Time evolution of the temperature for Vienna and Innsbruck

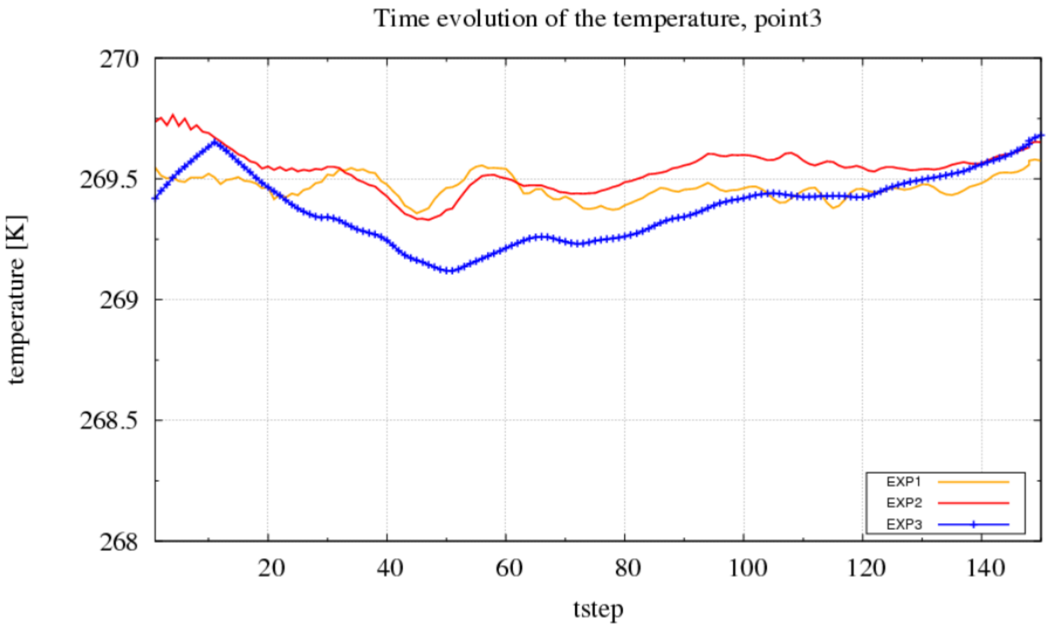

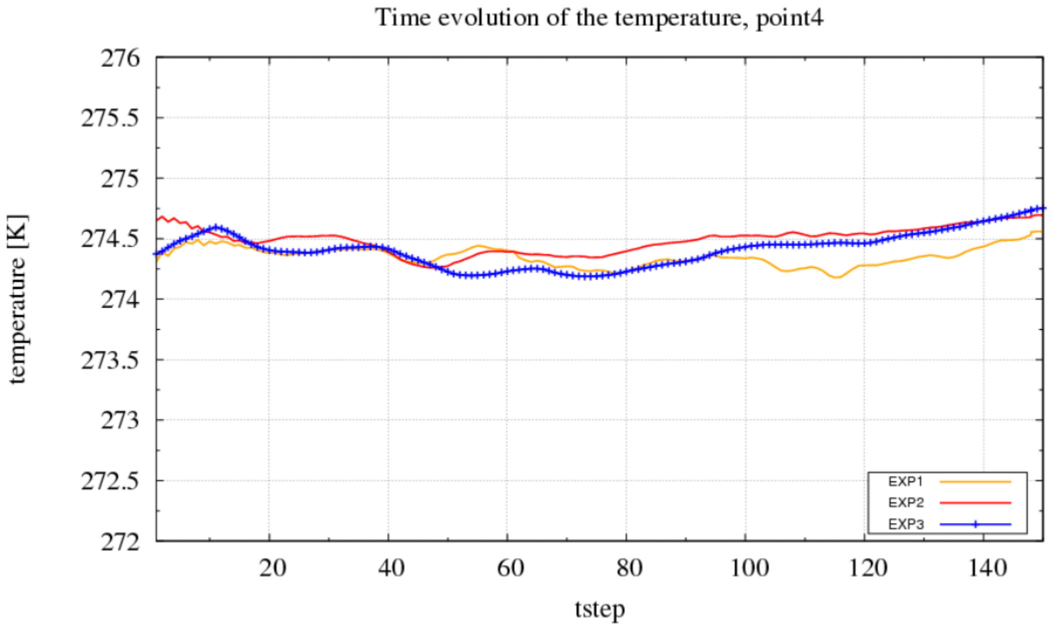

Figure 15: Time evolution of the temperature for Klagenfurt and Salzburg

Model Evaluation Tools (MET) was developed by the National Center for Atmospheric Research (NCAR) Developmental Testbed Center (DTC) through the grants from the National Science Foundation (NSF), The National Oceanic and Atmospheric Administration (NOAA), the United States Air Force (USAF), and the United States Department of Energy (DOE). NCAR is sponsored by the United States National Science Foundation.

Acknowledgements

I would like to thank to Christoph Wittmann, Florian Meier and Yong Wang for their constant help, advice and the entire support during my stay.

References

[1] http://www.cnrm-game-meteo.fr/aladin/IMG/pdf/aladinworkshop2016_florianmeier.pdf.

[2] Wolff, J., M. Harrold, T. Fowler, J. Halley-Gotway, L. Nance, and B. Brown, 2014: Beyond the basics: Evaluating model-based precipitation forecasts using traditional, spatial, and object-based methods. Wea. Forecasting, 29, 14511472, doi:https://doi.org/10.1175/WAF-D-13-00135.1

[3] Mittermaier MP, Bullock R. 2013. Using MODE to explore the spatial and temporal characteristics of cloud cover forecasts from high-resolution NWP models. Meteorol. Appl. 20: 187196 DOI: 10.1002/met.1393

[4] Davis C.A., B.G. Brown, and R.G. Bullock, 2006: Object based verification of precipitation forecasts, Part I: Methodology and application to mesoscale rain areas. Mon. Wea. Rev., 134, 1772-1784.

[5] Davis, C.A., B.G. Brown, R.G. Bullock and J. Halley Gotway, 2009: The Method for Object-based Diagnostic Evaluation (MODE) Applied to WRF Forecasts from the 2005 SPC Spring Program. Submitted to Weather and Forecasting; available at http://www.dtcenter.org/met/users/docs/overview.php.

[6] Cedilnik Jure, Study of spinup properties in AROME RUC 3DVAR, Mto France stay report, december 2007 https://www.umr-cnrm.fr/aladin/IMG/pdf/JureDec.pdf

[7] NOAA National Centers for Environmental Information, State of the Climate: Global Analysis for Annual 2016, published online January 2017, retrieved on September 11, 2017 from https://www.ncdc.noaa.gov/sotc/global/201613.